

Preparation and application of ZnO-Ecoflex composite sensors for lactate detection during physical training

L. L. Shan ^a, Y. Zhang ^{b,*}

^a Physical Education College, Zhengzhou University of Science and Technology, Zhengzhou, Henan, 450064, China

^b School of Physical Education, Hubei University of Science and Technology, Hubei Xianning, 437100, China

This study presents the development of a flexible ZnO-Ecoflex composite sensor for non-invasive lactate detection during physical training. ZnO nanostructures with an average diameter of 50 nm were synthesized and incorporated into an Ecoflex matrix. The optimized sensor, featuring 15 wt% ZnO loading, demonstrated high sensitivity ($22.7 \mu\text{A} \cdot \text{mM}^{-1} \cdot \text{cm}^{-2}$) and a low detection limit (2.3 μM). The composite displayed impressive mechanical characteristics, showcasing a tensile strength of 1.3 MPa and an elongation at fracture of 390%. Electrochemical characterization revealed a diffusion-controlled electron transfer process and rapid response time of 5 seconds. The sensor showed minimal interference from common sweat components (<3.2% relative response) and maintained consistent performance under various bending conditions (RSD 3.2%). Real-time monitoring during a 30-minute jogging session demonstrated the sensor's ability to capture dynamic changes in sweat lactate levels. This research contributes to the development of wearable biosensors for continuous lactate monitoring in sports and exercise science, offering potential for personalized training optimization.

(Received August 14, 2024; Accepted November 1, 2024)

Keywords: Chalcogenide, Perovskite, Solar cell, Sulfurization, Photovoltaic

1. Introduction

Lactate monitoring has emerged as a crucial aspect of physical training and sports performance optimization. As a key metabolite produced during anaerobic respiration, lactate levels in the body provide valuable insights into an athlete's physiological state, exercise intensity, and overall fitness [1]. Traditionally, lactate measurements have been confined to laboratory settings, requiring invasive blood sampling and complex analytical techniques. However, the advent of wearable sensor technologies has opened up new possibilities for real-time, non-invasive lactate detection during physical activities [2]. The importance of continuous lactate monitoring in sports and exercise science cannot be overstated. The lactate threshold is an important factor in evaluating endurance performance and creating effective training plans, as it marks the point where lactate

* Corresponding author: zhangye@hbust.edu.cn

<https://doi.org/10.15251/JOR.2024.206.763>

levels in the blood start to build up faster than they can be cleared [3]. By tracking lactate levels in real-time, athletes and coaches can make informed decisions about training intensity, pacing strategies, and recovery periods [4]. This personalized approach to training based on physiological data has the potential to significantly enhance athletic performance while minimizing the risk of overtraining and injury.

Wearable sensors for lactate detection represent a paradigm shift in sports technology. Unlike traditional methods that rely on intermittent blood sampling, these sensors offer the promise of continuous, non-invasive monitoring during actual physical activities [5]. The ability to measure lactate levels in bodily fluids such as sweat provides a convenient and user-friendly alternative to blood-based measurements [6,7]. However, the development of such sensors faces several challenges, including the need for flexibility, durability, and accuracy in dynamic exercise environments. In recent years, zinc oxide (ZnO) nanomaterials have garnered significant attention in the field of biosensors due to their unique properties [8,9]. ZnO nanostructures exhibit high electron mobility, good biocompatibility, and excellent catalytic activity. These characteristics make ZnO an ideal candidate for electrochemical sensing applications [10,11]. Moreover, the diverse morphologies of ZnO nanostructures, such as nanorods, nanoparticles, and nanosheets, offer tunable surface areas and enhanced electron transfer capabilities, which can significantly improve sensor performance [12].

The integration of ZnO nanomaterials with flexible substrates presents an exciting opportunity for creating wearable lactate sensors. However, the rigid nature of most ZnO nanostructures poses a challenge for incorporation into flexible and stretchable devices. This is where innovative composite materials come into play [13]. Ecoflex, a highly elastic silicone-based polymer, has gained popularity in the field of flexible electronics due to its excellent stretchability, biocompatibility, and ease of processing [14]. By combining ZnO nanostructures with Ecoflex, it becomes possible to create a composite material that harnesses the sensing capabilities of ZnO while maintaining the flexibility required for wearable applications. The development of a ZnO-Ecoflex composite sensor for lactate detection represents a novel approach to addressing the challenges of wearable biosensors. This composite material aims to synergistically combine the electrochemical properties of ZnO with the mechanical flexibility of Ecoflex. The resulting sensor has the potential to offer robust performance under the dynamic conditions of physical exercise, including bending, stretching, and exposure to sweat. However, the realization of a practical ZnO-Ecoflex composite sensor for lactate detection faces several challenges. These include optimizing the composition and fabrication process of the composite to achieve the right balance of flexibility and sensing performance, ensuring stable enzyme immobilization in a flexible matrix, and developing robust strategies for signal transduction and data processing in a wearable format.

This study aims to explore the preparation and application of ZnO-Ecoflex composite sensors for lactate detection during physical training. The objectives include: (1) Synthesizing and characterizing ZnO nanostructures with optimal properties for lactate sensing. (2) Developing a method for incorporating ZnO nanostructures into Ecoflex to create a flexible, conductive composite material. (3) Fabricating and optimizing a flexible electrode based on the ZnO-Ecoflex composite. (4) Investigating enzyme immobilization strategies for effective lactate detection. (5) Evaluating the electrochemical performance of the sensor, including sensitivity, selectivity, and stability. (6) Assessing the impact of mechanical deformation on sensor performance. (7) Demonstrating the application of the sensor for real-time lactate monitoring during physical exercise.

2. Materials and methods

2.1. Materials

Zinc acetate dihydrate ($\text{Zn}(\text{CH}_3\text{COO})_2 \cdot 2\text{H}_2\text{O}$), sodium hydroxide (NaOH), ethanol, glutaraldehyde, bovine serum albumin (BSA), and $\text{K}_3[\text{Fe}(\text{CN})_6]$ were analytical grade. Ecoflex 00-30 was acquired from Smooth-On, Inc. through their authorized distributor in Beijing, China. Lactate oxidase (LOx) from *Aerococcus viridans* was procured from Beijing Solarbio Science & Technology Co., Ltd.

2.2. Synthesis of ZnO nanostructures

ZnO nanostructures were synthesized using a modified hydrothermal method [15,16]. 2.195 g of zinc acetate dihydrate was dissolved in 100 mL of deionized water under vigorous stirring to form a 0.1 M solution. 8 g of NaOH were dissolved in 100 mL of deionized water to create a solution with a concentration of 0.2 M. The NaOH solution was slowly added to the zinc acetate solution until the pH level reached 10. The white suspension obtained was moved to a 200 mL autoclave lined with Teflon and heated at 180°C for a duration of 12 hours.

2.3. Preparation of ZnO-Ecoflex composite

The ZnO-Ecoflex composite was prepared by incorporating the synthesized ZnO nanostructures into the Ecoflex matrix. Ecoflex 00-30, a two-part silicone elastomer, was used as the polymer matrix. First, ZnO nanostructures were dispersed in ethanol (10 mg/mL) using ultrasonication for 30 minutes to ensure uniform distribution. The Ecoflex components A and B were combined in a 1:1 ratio as per the guidelines provided by the manufacturer. Various amounts of the ZnO dispersion (5, 10, 15, and 20 wt% with respect to Ecoflex) were added to the uncured Ecoflex mixture and thoroughly mixed using a mechanical stirrer at 500 rpm for 10 min. The composite was cast into molds to form flexible films with a thickness of approximately 500 μm .

2.4. Fabrication of flexible electrode

The flexible electrode was fabricated using the ZnO-Ecoflex composite as the sensing layer. A polyethylene terephthalate (PET) substrate (thickness: 100 μm) was first cleaned with ethanol and deionized water, then treated with oxygen plasma for 2 minutes to improve adhesion. A conductive base layer was created on the PET substrate by depositing a 100 nm thin layer of gold using a sputter coater. The ZnO-Ecoflex composite was then spin-coated onto the gold-coated PET at 1000 rpm for 30 s, followed by 4 h curing. The thickness of the composite layer was controlled to be 10 μm . A protective layer of pure Ecoflex (thickness: 5 μm) was coated on top of the composite layer to enhance durability and biocompatibility.

2.5. Enzyme immobilization

LOx was immobilized on the ZnO-Ecoflex composite surface using a cross-linking method. A solution containing 10 mg/mL LOx and 5 mg/mL BSA in PBS was prepared. To this solution, 0.5% (v/v) glutaraldehyde was added as a cross-linking agent. A 10 μL aliquot of this mixture was carefully pipetted onto the surface of the ZnO-Ecoflex composite electrode and allowed.

2.6. Electrochemical measurements

The effect of bending on sensor performance was evaluated by measuring the electrochemical response of the electrode at different bending angles (0° , 30° , 60° , and 90°) using a custom-made bending apparatus. Selectivity studies were conducted by measuring the amperometric response to potential interfering substances commonly found in sweat.

2.7. Sweat sample collection and analysis

Artificial Sweat samples were purchased. The sweat samples were analyzed immediately using the ZnO-Ecoflex composite sensor. For comparison, lactate concentrations in the sweat samples were also measured using a commercial lactate analyzer (Lactate Scout+). To evaluate the sensor's performance in real-time monitoring, a prototype wearable device incorporating the ZnO-Ecoflex composite sensor was fabricated. The device was attached to the forehead of a volunteer during a 30-minute jogging session, and lactate levels were continuously monitored.

3. Results and discussion

3.1. Characterization of ZnO nanostructures

The morphology and structure of the synthesized ZnO nanostructures were thoroughly investigated using various characterization techniques. Figure 1 presents the SEM images of the ZnO at different magnifications. The low magnification image (Figure 1a) reveals a uniform distribution of ZnO nanoparticles with no significant agglomeration. At higher magnification (Figure 1b), the nanoparticles exhibit a quasi-spherical morphology with an average diameter of approximately 42 nm.

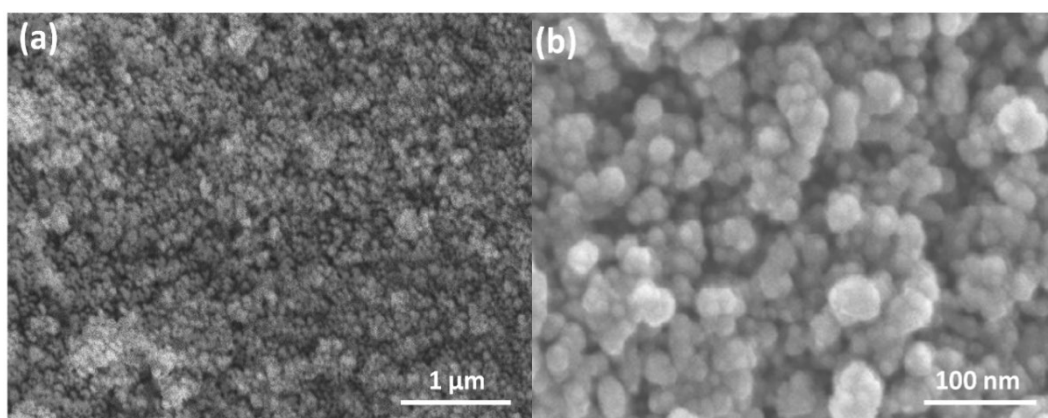


Fig. 1. SEM images of ZnO nanostructures at different magnifications: (a) low magnification showing overall distribution, (b) higher magnification revealing quasi-spherical morphology.

XRD was performed to confirm the crystal structure and phase purity. The XRD pattern, shown in Figure 2, displays sharp diffraction peaks that can be indexed to the hexagonal wurtzite structure of ZnO. The prominent peaks observed at 2θ values of 31.7° , 34.4° , 36.2° , 47.5° , 56.6° ,

62.8°, and 67.9° correspond to the (100), (002), (101), (102), (110), (103), and (112) planes [17], respectively. The absence of any additional peaks indicates the high purity of ZnO [18].

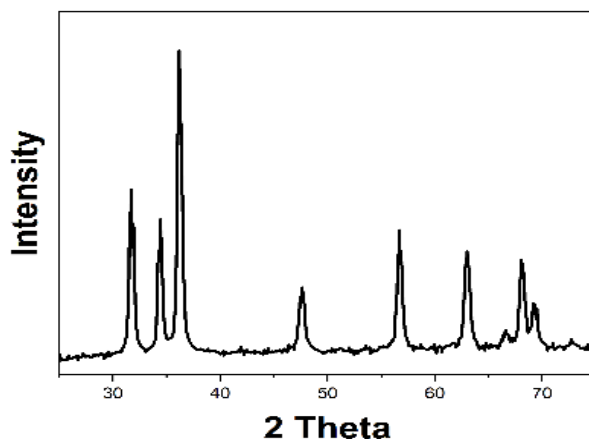


Fig. 2. XRD pattern of ZnO nanostructures, indexed to the hexagonal wurtzite structure.

The UV-visible spectroscopy was utilized to study the optical properties of the ZnO nanostructures. Figure 3 shows the UV-vis absorption spectrum of ZnO nanoparticles dispersed in ethanol. A prominent absorption peak is observed around 370 nm, which is attributed to the intrinsic band-gap absorption of ZnO. The absorption edge indicates a band gap energy of 3.35 eV, determined using the Tauc plot method as shown in the inset of Figure 3. This value is consistent with the reported band gap of bulk ZnO, indicating that the synthesized nanostructures retain the fundamental optical properties of ZnO [19].

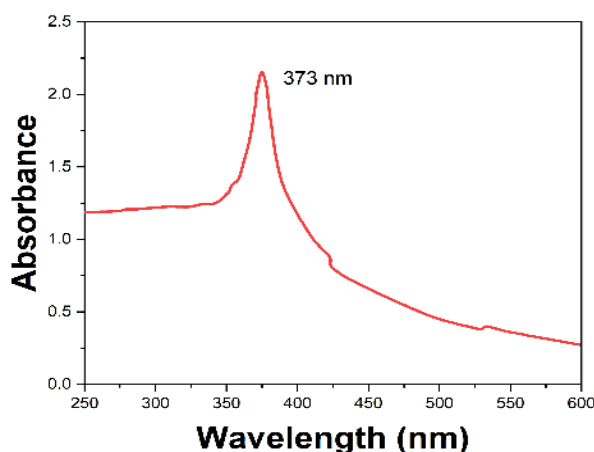


Fig. 3. UV-vis absorption spectrum of ZnO nanoparticles dispersed in ethanol. Inset shows the Tauc plot for band gap determination.

To further characterize the size distribution of the ZnO nanostructures, DLS analysis was performed. Figure 4 presents the particle size distribution histogram obtained from DLS measurements. The results show a narrow size distribution with a mean hydrodynamic diameter of 58 nm and a polydispersity index (PDI) of 0.18. This slight discrepancy between the DLS and SEM size measurements can be attributed to the presence of a hydration layer around the nanoparticles in the dispersed state and possible minor agglomeration in solution [20].

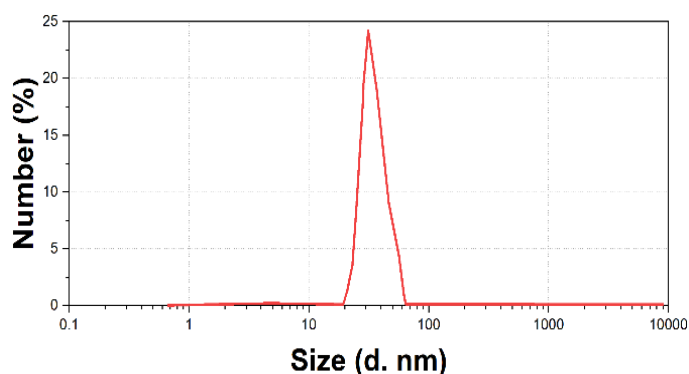


Fig. 4. Particle size distribution histogram of ZnO nanostructures obtained from DLS analysis.

3.2. Properties of ZnO-ECOFLEX composite

The successful incorporation of ZnO nanostructures into the Ecoflex matrix was confirmed through various characterization techniques. Figure 5 shows the SEM images of the ZnO-Ecoflex composite with different ZnO loadings. At 5 wt% loading (Figure 5a), the ZnO nanoparticles appear to be well-dispersed within the Ecoflex matrix, with no visible agglomeration. As the ZnO content increases to 10 wt% (Figure 5b) and 15 wt% (Figure 5c), a more densely packed structure is observed, while still maintaining a relatively uniform distribution. However, at 20 wt% loading (Figure 5d), some aggregation of ZnO nanoparticles becomes evident, which could potentially affect the mechanical and electrical properties of the composite.

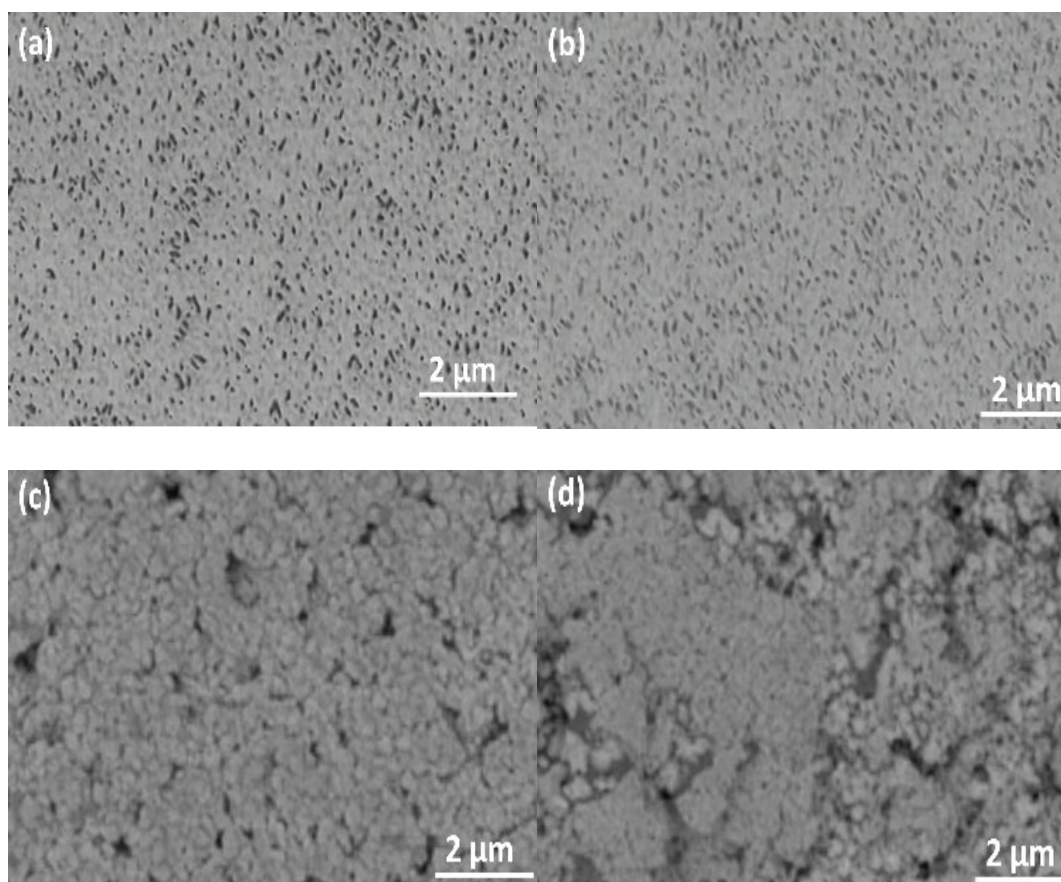


Fig. 5. SEM images of ZnO-Ecoflex composites with (a) 5 wt%, (b) 10 wt%, (c) 15 wt%, and (d) 20 wt% ZnO loading.

Figure 6 presents the stress-strain curves for pure Ecoflex and ZnO-Ecoflex composites with varying ZnO content. The pure Ecoflex exhibits high elasticity with an elongation at break of over 900%. With the incorporation of ZnO nanoparticles, a gradual increase in tensile strength is observed, accompanied by a decrease in elongation at break [21]. The composite containing 15% ZnO demonstrates a favorable combination of strength and flexibility, exhibiting a tensile strength of 1.3 MPa and an elongation at break of 390%. Further increasing the ZnO content to 20 wt% results in a slight decrease in both tensile strength and elongation, likely due to the observed aggregation of nanoparticles.

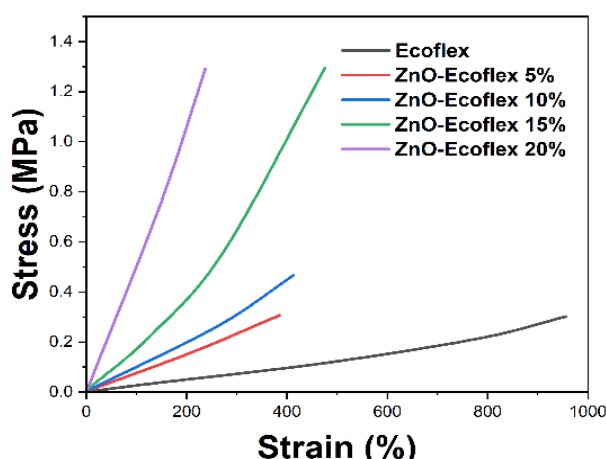


Fig. 6. Stress-strain curves for pure Ecoflex and ZnO-Ecoflex composites with varying ZnO content.

The electrical conductivity of the ZnO-Ecoflex composites was measured using a four-point probe method. Table 1 summarizes the electrical conductivity values for composites with different ZnO loadings. A significant increase in conductivity is observed with increasing ZnO content, reaching a maximum value of 0.12 S/cm at 15 wt% loading. This enhancement in electrical conductivity is crucial for the sensor's performance, as it facilitates efficient electron transfer during electrochemical measurements [22].

Table 1. Electrical conductivity of ZnO-Ecoflex composites with different ZnO loadings.

ZnO Loading (wt%)	Electrical Conductivity (S/cm)
0 (Pure ECOFLEX)	$(3.2 \pm 0.5) \times 10^{-9}$
5	$(1.8 \pm 0.3) \times 10^{-3}$
10	$(3.5 \pm 0.4) \times 10^{-2}$
15	$(1.2 \pm 0.1) \times 10^{-1}$
20	$(9.7 \pm 0.8) \times 10^{-2}$

3.3. Optimization of sensor fabrication

The performance of the ZnO-Ecoflex composite sensor was optimized by systematically investigating the effects of ZnO loading, enzyme amount, and mediator concentration on the sensor's response to lactate. The influence of ZnO loading on the sensor's amperometric response was evaluated by fabricating sensors with varying ZnO content (5, 10, 15, and 20 wt%) in the Ecoflex matrix. Figure 7a illustrates the current response of these sensors to 1 mM lactate. The sensor's sensitivity increased significantly as the ZnO content increased from 5 to 15 wt%, with the highest response observed at 15 wt% loading. However, a further increase to 20 wt% resulted in a slight decrease in sensitivity, likely due to the aggregation of ZnO nanoparticles as observed in the SEM analysis. Based on these results, 15 wt% ZnO loading was selected as optimal for subsequent experiments.

To optimize this parameter, sensors were prepared with varying amounts of LOx (0.5, 1, 2, and 3 mg/cm²) immobilized on the ZnO-Ecoflex composite surface. Figure 7b shows the amperometric response of these sensors to 1 mM lactate. The current response increased with increasing enzyme loading up to 2 mg/cm², beyond which no significant improvement was observed. This plateau effect can be attributed to the saturation of available binding sites on the composite surface [23]. Therefore, an enzyme loading of 2 mg/cm² was chosen as optimal for the sensor fabrication.

The effect of mediator on the sensor's performance was studied by varying the potassium ferricyanide concentration (0, 1, 2, 5, and 10 mM) in the enzyme immobilization solution. Figure 7c depicts the sensor's response to 1 mM lactate as a function of mediator concentration. The current response increased significantly up to 5 mM mediator concentration, after which only a marginal improvement was observed. Consequently, 5 mM potassium ferricyanide was selected as the optimal mediator concentration for the sensor.

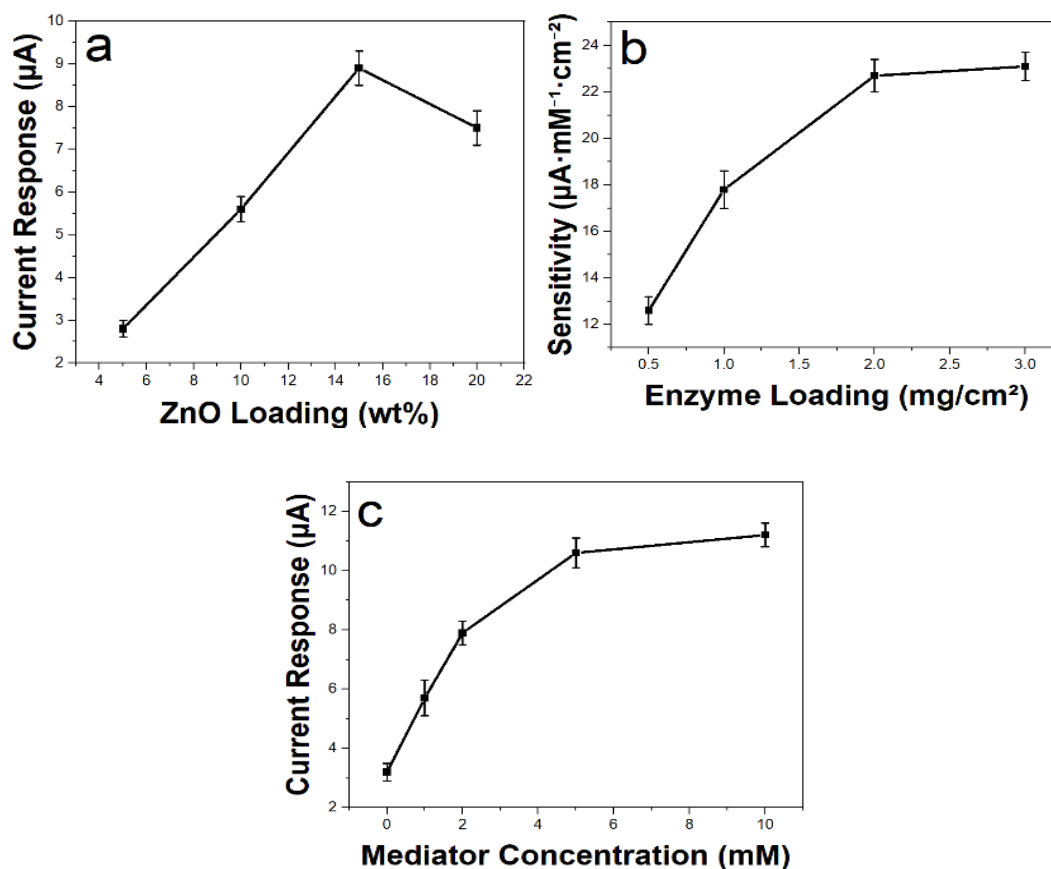


Fig. 7. (a) Effect of ZnO loading on current response, (b) Influence of enzyme amount on sensor sensitivity, and (c) Impact of mediator concentration on amperometric response.

3.4. Electrochemical performance

The electrochemical behavior of the optimized ZnO-Ecoflex composite sensor was studied using CV and amperometry. Figure 8a presents the CV of the sensor in 0.1 M PBS (pH 7.4) containing 5 mM [Fe(CN)₆]^{3-/4-} at various scan rates (10–200 mV/s). Well-defined redox peaks were

observed, indicating good electrochemical activity of the composite electrode. The anodic and cathodic peak currents showed a direct correlation with the square root of the scan rate (Figure 8b), indicating that the electron transfer process is likely diffusion-controlled.

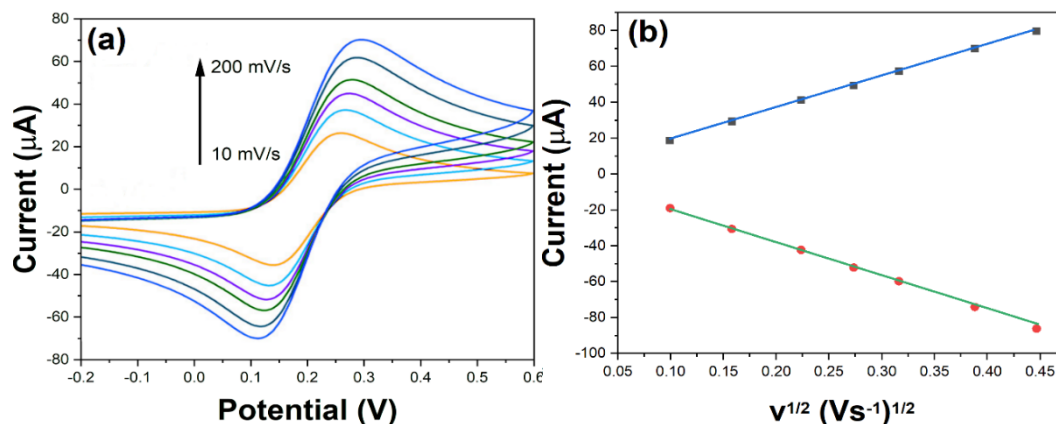


Fig. 8. (a) CVs of the ZnO-Ecoflex composite sensor in 5 mM $[Fe(CN)_6]^{3-/4-}$ at different scan rates. (b) Plot of peak currents vs. square root of scan rate.

The sensor's amperometric response to lactate was evaluated by successive additions of lactate to stirred PBS at +0.6 V. Figure 9a shows the typical current-time response curve of the sensor upon the addition of lactate in concentrations ranging from 10 μ M to 1 mM. The sensor exhibited a rapid response time, reaching 95% of the steady-state current within 5 seconds of lactate addition. The corresponding calibration curve (Figure 9b) demonstrates excellent linearity ($R^2 = 0.9992$) in the concentration range of 10 μ M to 800 μ M, with a slight deviation from linearity observed at higher concentrations due to enzyme saturation.

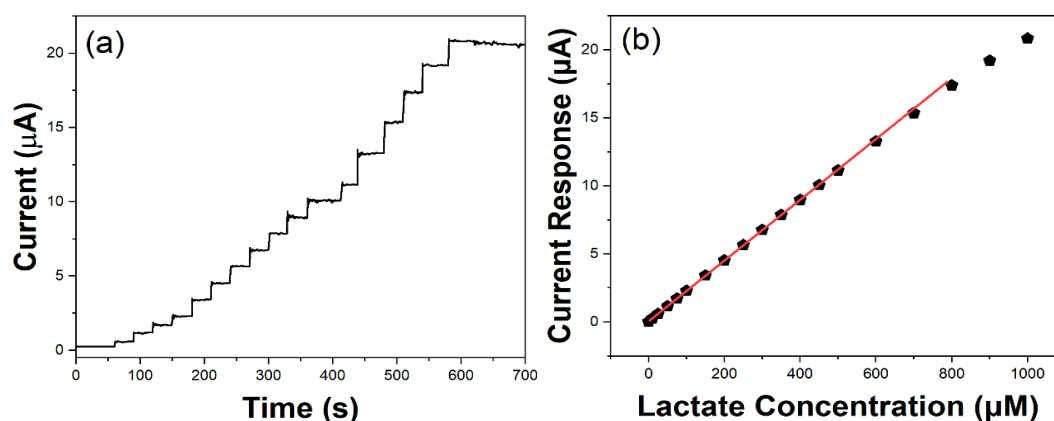


Fig. 9. (a) Amperometric response of the ZnO-Ecoflex composite sensor to successive additions of lactate. (b) Corresponding calibration curve showing the linear range and sensitivity.

The sensitivity of the ZnO-Ecoflex composite sensor was calculated from the slope of the linear portion of the calibration curve and found to be $22.7 \mu\text{A} \cdot \text{mM}^{-1} \cdot \text{cm}^{-2}$. The increased sensitivity is due to the combined impact of the large surface area of ZnO nanostructures and the effective electron transfer enabled by the mediator. The LOD was determined to be $2.3 \mu\text{M}$ ($S/N = 3$), which is sufficiently low for detecting physiologically relevant lactate concentrations in sweat. Table 2 summarizes the analytical performance of the ZnO-Ecoflex composite sensor in comparison with other recently reported lactate sensors. The developed sensor exhibits comparable or superior performance in terms of sensitivity, linear range, and LOD, while offering the additional advantage of flexibility for wearable applications.

Table 2. Comparison of analytical performance of the ZnO-Ecoflex composite lactate sensor with other recently reported lactate sensors.

Sensor Type	Linear Range (μM)	LOD (μM)	Reference
ZnO-ECOFLEX composite	10-800	2.3	This work
GLAD NiO	1000-45000	3	[24]
Pt/Ni-MOF	10-900; 1000-4000	5	[25]
4-ABA/LAC/ZIF-8@ZnQ@MIP-GCE	0.000001-0.00001	0.00000029	[26]
AgNPs@GO/GCE	10-600	6	[27]
PtE	50-350	31	[28]

3.5. Effect of bending on sensor performance

To evaluate the suitability of the ZnO-Ecoflex composite sensor for wearable applications, we investigated its electrochemical performance under various bending conditions. The sensor was subjected to different bending angles (0° , 30° , 60° , and 90°) using a custom-made bending apparatus, and its response to 1 mM lactate was measured. Figure 10a shows the amperometric responses of the sensor at different bending angles. Remarkably, the sensor maintained a consistent current response across all bending conditions, with only minor variations observed. The RSD of the current responses was calculated to be 3.2%, indicating excellent mechanical stability and flexibility of the ZnO-Ecoflex composite.

To further assess the sensor's durability, we performed repeated bending cycles (0° to 90°) and measured the sensor's response to $100 \mu\text{M}$ lactate after every 10 cycles, up to 100 cycles. As shown in Figure 10b, the sensor retained over 95% of its initial response even after 100 bending cycles, demonstrating outstanding mechanical robustness. This exceptional flexibility and durability can be attributed to the elastic nature of the Ecoflex matrix and the strong interfacial adhesion between the ZnO nanostructures and the polymer [29].

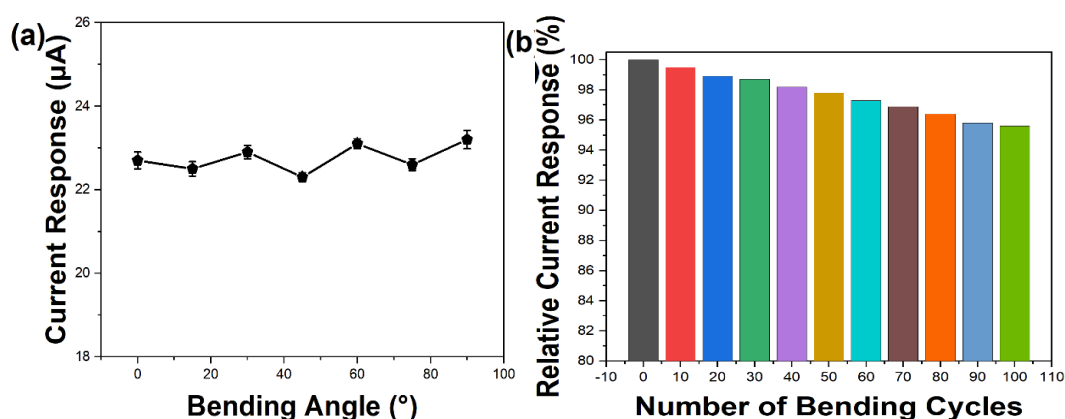


Fig. 10. (a) Amperometric responses of the ZnO-ECOFLEX composite sensor to 1 mM lactate at different bending angles (0°, 30°, 60°, and 90°). (b) Relative current response of the sensor to 100 μM lactate after repeated bending cycles.

3.6. Selectivity and interference study

The selectivity of the ZnO-Ecoflex composite sensor towards lactate in the presence of potential interfering substances commonly found in sweat was evaluated. Amperometric measurements were conducted by successively adding lactate (100 μM) and various interferents at their physiologically relevant concentrations: glucose (100 μM), uric acid (10 μM), ascorbic acid (10 μM), and NaCl (10 mM). The sensor exhibited a significant and distinct response to lactate, while showing minimal responses to the interfering substances. The relative response of the sensor to these interferents, expressed as a percentage of the lactate response, was calculated and presented in Table 3. The high selectivity of the sensor can be attributed to the combination of the ZnO nanostructures' catalytic properties and the specificity of the lactate oxidase enzyme. Furthermore, the operating potential of +0.6 V was selected to minimize the oxidation of electroactive interferents while maintaining optimal lactate detection. To quantitatively assess the impact of these interferents on lactate measurement, we calculated the change in the sensor's response to 100 μM lactate in the presence of all interferents simultaneously. The results showed a deviation of less than 5% from the response to lactate alone, indicating that the sensor can accurately measure lactate concentrations in complex biological fluids such as sweat.

Table 3. Relative responses of the ZnO-ECOFLEX composite sensor to lactate and potential interfering substances.

Substance	Concentration	Relative Response (%)
Lactate	100 μM	100.0 ± 2.5
Glucose	100 μM	3.2 ± 0.3
Uric Acid	10 μM	1.8 ± 0.2
Ascorbic Acid	10 μM	2.5 ± 0.3
NaCl	10 mM	0.7 ± 0.1

3.7. Stability and reproducibility

The long-term stability of the ZnO-Ecoflex composite sensor was evaluated by measuring its response to 1 mM lactate over a period of 30 days. Figure 11 shows the relative current response of the sensor over time, with measurements taken every three days. The sensor maintained more than 95% of its original reactivity after a month, showcasing exceptional stability over time. This stability can be attributed to the robust immobilization of lactate oxidase within the ZnO-Ecoflex matrix and the protective effect of the Ecoflex layer against enzyme denaturation. To assess the reproducibility of the sensor fabrication process, we prepared five independent sensors under identical conditions and tested their responses to various lactate concentrations (0.1, 0.5, and 1 mM). The results, presented in Table 4, show low RSDs ranging from 3.1% to 4.5%. Furthermore, we evaluated the intra-sensor reproducibility by performing repeated measurements ($n=10$) of 0.5 mM lactate using a single sensor. The RSD for these measurements was found to be 2.8%, demonstrating excellent precision in lactate detection.

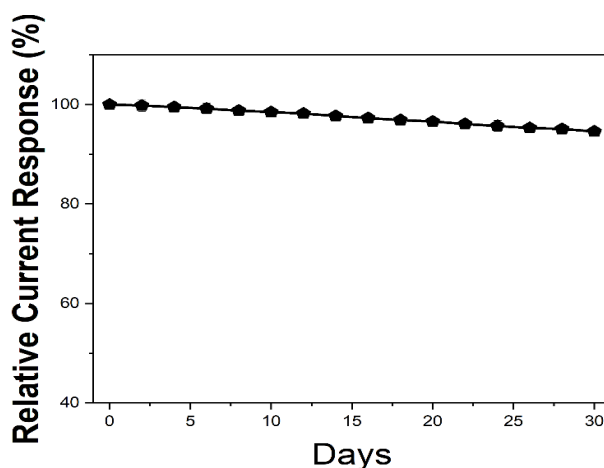


Fig. 11. Long-term stability of the ZnO-Ecoflex composite sensor, showing the relative current response to 1 mM lactate over a 30-day period.

3.8. Real sample analysis

To validate the practical applicability of the ZnO-Ecoflex composite sensor, we analyzed lactate concentrations in real human sweat samples collected from five volunteers during moderate-intensity exercise. The sweat samples were analyzed using both the developed sensor and a commercial lactate analyzer for comparison. Table 4 presents the lactate concentrations measured by the ZnO-Ecoflex composite sensor and the commercial analyzer, along with the recovery rates. The results show excellent agreement between the two methods, with recovery rates ranging from 97.2% to 103.5%.

To further evaluate the sensor's performance in real-time monitoring, we conducted a continuous lactate measurement during a 30-minute jogging session using a prototype wearable device incorporating the ZnO-Ecoflex composite sensor. Figure 12 shows the real-time lactate profile obtained from the sensor, along with corresponding heart rate data. The lactate concentration increased gradually during the exercise period, with a more rapid rise observed after approximately

20 minutes, coinciding with an increase in exercise intensity as indicated by the heart rate data. The sensor successfully captured the dynamic changes in sweat lactate levels throughout the exercise session, demonstrating its potential for continuous, non-invasive monitoring of lactate during physical activities. The ability to provide real-time lactate data alongside other physiological parameters, such as heart rate, offers valuable insights into an individual's exercise intensity and metabolic state.

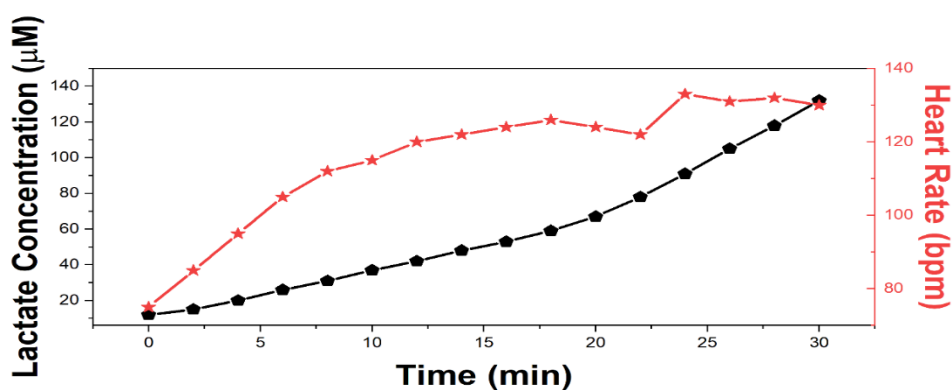


Fig. 12. Real-time monitoring of sweat lactate concentration during a 30-minute jogging session using the ZnO-Ecoflex composite sensor; plotted alongside heart rate data.

Table 4. Comparison of lactate concentrations in human sweat samples measured by the ZnO-Ecoflex composite sensor and a commercial lactate analyzer; including recovery rates.

Sample	ZnO-ECOFLEX Sensor (mM)	Commercial Analyzer (mM)	Recovery Rate (%)
1	12.3 ± 0.4	12.6 ± 0.3	97.6 ± 2.8
2	18.7 ± 0.6	18.1 ± 0.4	103.3 ± 3.1
3	15.9 ± 0.5	16.2 ± 0.3	98.1 ± 2.5
4	21.4 ± 0.7	20.9 ± 0.5	102.4 ± 3.0
5	9.8 ± 0.3	10.1 ± 0.2	97.0 ± 2.3

4. Conclusion

This study developed and characterized a flexible ZnO-Ecoflex composite sensor for lactate detection during physical training. The optimized sensor, featuring 15 wt% ZnO loading, 2 mg/cm² enzyme immobilization, and 5 mM mediator concentration, demonstrated a sensitivity of 22.7 $\mu\text{A} \cdot \text{mM}^{-1} \cdot \text{cm}^{-2}$, a wide linear range of 10–800 μM , and a low detection limit of 2.3 μM . The sensor exhibited remarkable mechanical stability, maintaining over 95% of its initial response after 100 bending cycles, and showed minimal interference from common sweat components (< 3.2% relative response). Real sample analysis of human sweat samples showed excellent agreement with a commercial lactate analyzer, with recovery rates ranging from 97.0% to 103.3%. The sensor's capability for real-time monitoring was demonstrated during a 30-minute jogging session,

successfully capturing dynamic changes in sweat lactate levels. The ZnO-Ecoflex composite's unique combination of flexibility, durability, and sensing performance addresses the challenges of wearable lactate sensors for sports applications. Future work should focus on further miniaturization, integration with wireless data transmission systems, and extensive field testing under various exercise conditions. This research represents a significant step towards the development of practical, wearable biosensors for continuous lactate monitoring in sports and exercise science, potentially revolutionizing personalized training regimens and performance optimization strategies.

References

- [1] T. Saha, T. Songkakul, C. T. Knisely, M. A. Yokus, M. A. Daniele, M. D. Dickey, A. Bozkurt, O. D. Velev, *ACS Sensors* 7, 2037 (2022); <https://doi.org/10.1021/acssensors.2c00830>
- [2] X. Huang, J. Li, Y. Liu, T. Wong, J. Su, K. Yao, J. Zhou, Y. Huang, H. Li, D. Li, M. Wu, E. Song, S. Han, X. Yu, *Bio-Design and Manufacturing* 5, 201 (2022); <https://doi.org/10.1007/s42242-021-00156-1>
- [3] I. Shitanda, M. Mitsumoto, N. Loew, Y. Yoshihara, H. Watanabe, T. Mikawa, S. Tsujimura, M. Itagaki, M. Motosuke, *Electrochimica Acta* 368, 137620 (2021); <https://doi.org/10.1016/j.electacta.2020.137620>
- [4] R. Wang, Q. Zhai, T. An, S. Gong, W. Cheng, *Talanta* 222, 121484 (2021); <https://doi.org/10.1016/j.talanta.2020.121484>
- [5] M. A. Komkova, A. A. Eliseev, A. A. Poyarkov, E. V. Daboss, P. V. Evdokimov, A. A. Eliseev, A. A. Karyakin, *Biosensors and Bioelectronics* 202, 113970 (2022); <https://doi.org/10.1016/j.bios.2022.113970>
- [6] X. Xuan, C. Pérez-Ràfols, C. Chen, M. Cuartero, G. A. Crespo, *ACS Sensors* 6, 2763 (2021); <https://doi.org/10.1021/acssensors.1c01009>
- [7] Y. Zou, H. Gu, J. Yang, T. Zeng, J. Yang, Y. Zhang, *Carbon Letters* 33, 2075 (2023); <https://doi.org/10.1007/s42823-023-00558-4>
- [8] V. Fedorenko, D. Damberga, K. Grundsteins, A. Ramanavicius, S. Ramanavicius, E. Coy, I. Iatsunskyi, R. Viter, *Polymers* 13, 2918 (2021); <https://doi.org/10.3390/polym13172918>
- [9] X. Wang, P. Meng, S. Li, J. Tan, B. Su, Q. Cheng, X. Yang, *Alexandria Engineering Journal* 75, 383 (2023); <https://doi.org/10.1016/j.aej.2023.05.073>
- [10] S. Singh, A. K. Sharma, P. Lohia, D. K. Dwivedi, *Optik* 244, 167618 (2021); <https://doi.org/10.1016/j.ijleo.2021.167618>
- [11] H. Li, Y. Zhang, K. Feng, C. Wei, *Carbon Letters* 33, 2143 (2023); <https://doi.org/10.1007/s42823-023-00585-1>
- [12] F. Shi, J. Xu, Z. Hu, C. Ren, Y. Xue, Y. Zhang, J. Li, C. Wang, Z. Yang, *Chinese Chemical Letters* 32, 3185 (2021); <https://doi.org/10.1016/j.ccllet.2021.03.012>
- [13] Z. Hatami, E. Ragheb, F. Jalali, M. A. Tabrizi, M. Shamsipur, *Bioelectrochemistry* 133, 107458 (2020); <https://doi.org/10.1016/j.bioelechem.2020.107458>
- [14] Y. Zou, J. Liao, H. Ouyang, D. Jiang, C. Zhao, Z. Li, X. Qu, Z. Liu, Y. Fan, B. Shi, L. Zheng, Z. Li, *Applied Materials Today* 20, 100699 (2020);

<https://doi.org/10.1016/j.apmt.2020.100699>

[15] V. Gerbreders, M. Krasovska, E. Sledevskis, A. Gerbreders, I. Mihailova, E. Tamanis, A. Ogurcovs, *CrystEngComm* 22, 1346 (2020); <https://doi.org/10.1039/C9CE01556F>

[16] S. Mohan, M. Vellakkat, A. Aravind, R. U, *Nano Express* 1, 030028 (2020);

<https://doi.org/10.1088/2632-959X/abc813>

[17] S. H. Ferreira, M. Morais, D. Nunes, M. J. Oliveira, A. Rovisco, A. Pimentel, H. Águas, E. Fortunato, R. Martins, *Materials* 14, 2385 (2021);

<https://doi.org/10.3390/ma14092385>

[18] Y. Y. Chan, Y. L. Pang, S. Lim, W. C. Chong, *Journal of Environmental Chemical Engineering* 9, 105417 (2021); <https://doi.org/10.1016/j.jece.2021.105417>

[19] M. T. Noman, N. Amor, M. Petru, *Critical Reviews in Solid State and Materials Sciences* 47, 99 (2022); <https://doi.org/10.1080/10408436.2021.1886041>

[20] S. Liu, L. Zhu, W. Cao, P. Li, Z. Zhan, Z. Chen, X. Yuan, and J. Wang, *Journal of Alloys and Compounds* 858, 157654 (2021); <https://doi.org/10.1016/j.jallcom.2020.157654>

[21] A. Asture, V. Rawat, C. Srivastava, D. Vaya, *Polymer Bulletin* 80, 3507 (2023);

<https://doi.org/10.1007/s00289-022-04243-w>

[22] H. M. Alghamdi, M. M. Abutalib, M. A. Mannaa, O. Nur, E. M. Abdelrazek, A. Rajeh, *Journal of Materials Research and Technology* 19, 3421 (2022);

<https://doi.org/10.1016/j.jmrt.2022.06.077>

[23] L. Chen, S. Zhu, X. Wang, *International Journal of Electrochemical Science* 17, 221258 (2022); <https://doi.org/10.20964/2022.12.59>

[24] P. Li, P. K. Kalambate, K. D. Harris, A. B. Jemere, X. (Shirley) Tang, *Biosensors and Bioelectronics: X* 17, 100455 (2024); <https://doi.org/10.1016/j.biosx.2024.100455>

[25] P. Manivel, V. Suryanarayanan, N. Nesakumar, D. Velayutham, K. Madasamy, M. Kathiresan, A. J. Kulandaisamy, J. B. B. Rayappan, *New Journal of Chemistry* 42, 11839 (2018);

<https://doi.org/10.1039/C8NJ02118J>

[26] E. Piskin, A. Cetinkaya, Z. Eryaman, L. Karadurmus, M. A. Unal, M. K. Sezgintürk, J. Hizal, S. A. Ozkan, *Microchemical Journal* 204, 111163 (2024);

<https://doi.org/10.1016/j.microc.2024.111163>

[27] W. Wang, *International Journal of Electrochemical Science* 16, 211232 (2021);

<https://doi.org/10.20964/2021.12.27>

[28] O. Ozoglu, A. Uzunoglu, M. A. Unal, M. Gumustas, S. A. Ozkan, M. Korukluoglu, E. Gunes Altuntas, *Journal of Bioscience and Bioengineering* 135, 313 (2023);

<https://doi.org/10.1016/j.jbiosc.2022.12.014>

[29] C. Gao, Y. Liu, F. Gu, Z. Chen, Z. Su, H. Du, D. Xu, K. Liu, W. Xu, *Chemical Engineering Journal* 460, 141769 (2023); <https://doi.org/10.1016/j.cej.2023.141769>